

UNCLASSIFIED

Defense Technical Information Center
Compilation Part Notice

ADP012106

TITLE: Investigation of the Structure of a Reacting Hydrocarbon-Air
Planar Mixing Layer

DISTRIBUTION: Approved for public release, distribution unlimited

This paper is part of the following report:

TITLE: Army Research Office and Air Force Office of Scientific Research.
Contractors' Meeting in Chemical Propulsion [2001] Held in the University
of Southern California on June 18-19, 2001

To order the complete compilation report, use: ADA401046

The component part is provided here to allow users access to individually authored sections
of proceedings, annals, symposia, etc. However, the component should be considered within
the context of the overall compilation report and not as a stand-alone technical report.

The following component part numbers comprise the compilation report:
ADP012092 thru ADP012132

UNCLASSIFIED

INVESTIGATION OF THE STRUCTURE OF A REACTING HYDROCARBON-AIR PLANAR MIXING LAYER

Grant/Contract Number: DAAH04-94-G-0328.

Principal Investigator(s): Corradini, Farrell, Foster, Ghandhi, Reitz, Rutland

Engine Research Center
University of Wisconsin-Madison
1500 W. Engineering Dr.
Madison, WI 53706

SUMMARY

Mixing-controlled combustion of a hydrocarbon-air system was investigated experimentally in a planar two-stream mixing layer using planar laser-induced fluorescence of OH for visualization of the reaction zone, and planar LII of soot, which was found to effectively mark the edge of the parent fuel entrainment. The high-temperature combustion was found to locate on the lean reactant (air) side of the mixing layer, and was minimally perturbed by the fluid motion, resulting in the formation of an 'internal' mixing layer, reminiscent of a non-reacting mixing layer, between the combustion products and the neat fuel stream. For the same inlet hydrodynamic conditions, the large-scale structure spacing was found to decrease when the high-speed stream contained the fuel, whereas air as the high-speed fluid resulted in a lengthening of the structure spacing compared to non-reacting conditions. The effective density ratio established by the high temperature reaction zone located on the air side of the mixing layer is believed to be the cause for this behavior. A tripped high-speed boundary layer was found to have a large effect on non-reacting passive scalar measurements, but was not found to affect the mixing layer structure under reacting conditions, suggesting that the heat release serves to make the Kelvin-Helmholtz instability dominant.

TECHNICAL DISCUSSION

The latter stages of Diesel combustion are limited by the mixing of the partially oxidized products with the available air in the time available. High power density operation requires the mixing times to be quite short to enable the energy release due to combustion to be realized by the piston expansion, however for low particulate operation the time scale of importance is the time for the exhaust valve to open, significantly longer. The investigation of these processes in realistic engines is complicated by the high pressures, temperatures and the strong luminosity of the combusted gases. Additionally, modeling of the late-stage combustion is limited by the relative simplicity of the chemistry included in multi-dimensional models, which is required to facilitate the computation of this difficult flow. Thus, in order to develop a better fundamental understanding of mixing-controlled combustion under controlled conditions, a planar shear layer has been constructed.

A schematic of the shear layer apparatus is shown in Figure 1. Air (possibly heated), at the left, and a mixture of fuel and argon, at the right, pass through a series of flow conditioning

elements, consisting of perforated plates, tube bundles, and mesh screens, which reduce the turbulence level and isolate upstream acoustical modes from the shear layer. The streams meet at the tip of a splitter plate where they mix and react in an optically accessible test section. A symmetrical nozzle producing a 1.75:1 contraction ratio and a 3.8° tapered splitter plate (nominal tip thickness is 0.1 mm) were used to create the shear flow. The velocity profile at the splitter plate tip was measured to be uniform within 1.3%, with turbulence intensities < 0.5%. The test section downstream of the splitter plate was 5 cm in the cross-stream direction and 20 cm in the spanwise direction. The test section had two hinged walls that could be adjusted to eliminate the streamwise pressure gradient in the flow. For reacting experiments, the walls were extended 2° from the vertical position. The entire flow conditioning run and test section were enclosed in a pressurized containment vessel designed for operation at pressures up to 6 atm. Optical access was provided with fused silica windows at each quadrant of the test section and containment vessel. At the top of the containment vessel, the exhaust and slave gases were throttled to atmospheric pressure and then cooled and further diluted in a water quench tower before entering the laboratory exhaust system. The mixing layer was ignited with a swirl-stabilized ignitor mounted flush with the side wall. With reaction engaged in the mixing layer and the proper system pressure and flow rates established, the ignitor was shut off, leaving the mixing layer to sustain combustion on its own accord, undisturbed by the perturbation of the ignitor.

Planar LIF of OH was accomplished with a Nd:YAG pumped dye laser whose output was frequency doubled to 283.92 nm to pump the overlapping $Q_1(8)$ and $Q_2(9)$ lines of the $A^2\Sigma^+ \leftarrow X^2\Pi(1,0)$ band of OH. Figure 2 shows sample images acquired position B (see Fig. 1). Fig 2.a was obtained with the laser tuned on the OH transition while Fig. 2.b was obtained with the laser tuned off the OH line (283.75 nm). The filtering scheme allowed significant transmission from 310 - 358 nm. Comparison of the online and offline images clearly indicates that the strong signal at the left is OH, while the fainter signal to the right originates from a different, laser-excited source. To investigate whether this signal arose from particulate matter or polycyclic aromatic hydrocarbons (PAHs) which have broadband absorption and emission characteristics, elastic scatter images were collected, see Fig. 2.c. The strong similarity between the elastic scattering and offline images suggests that the source of the offline signal is scattering from particulate matter and not fluorescence. The spectral shift of the offline interference signal and its coincidence with the elastic scattering suggests that the source of the offline signal is laser-induced incandescence (LII) from soot particles. However, it is not possible to exclude the possibility of PAH fluorescence from the spatial locations where the soot exists.

To further investigate the nature of the signal originating from the soot particles, the fuel/argon stream was visualized by seeding the stream with (~2 % by volume) acetone and performing PLIF under

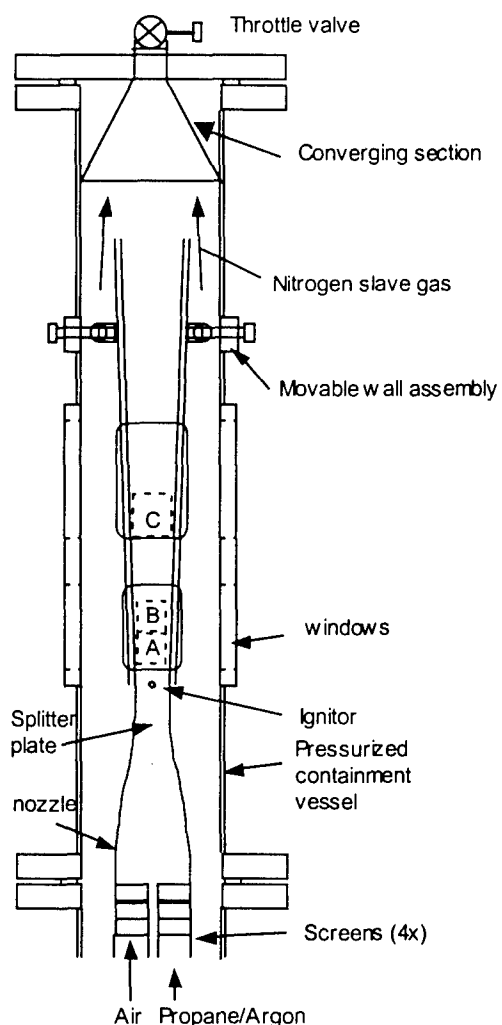


Figure 1 Shear layer apparatus

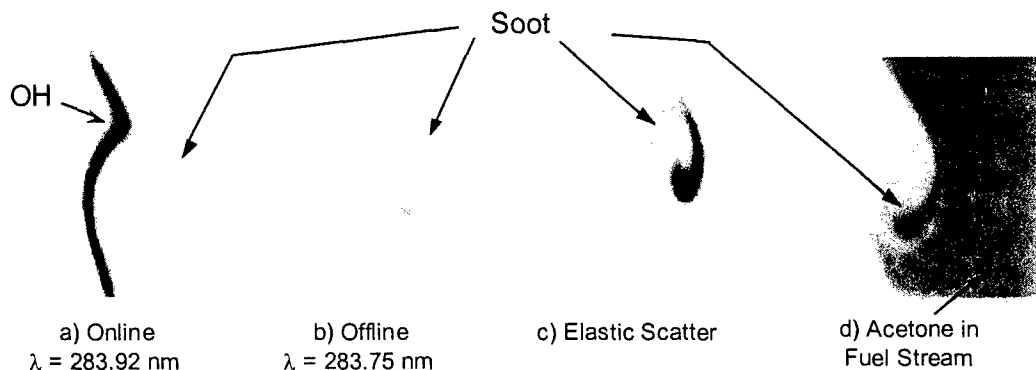


Figure 2 Signals obtained under reacting conditions with the high speed stream containing air ($U_1=2$ m/s, $T_1=400$ K) at the left and the low-speed stream containing 40% DME and 60% argon ($U_2=0.8$ m/s, $T_2=300$ K) at the right. Dark regions indicate stronger signals.

reacting conditions with the laser tuned off the OH transition, see Fig. 2.d. The acetone PLIF filtering scheme does not discriminate broadband fluorescence from LII. In Fig. 2.d the flat field of uniform intensity at the right is the acetone fluorescence. Near the core of the vortex there is a high intensity signal that is spatially separated from the acetone fluorescence. Based on the previous findings, it is believed that this is the LII signal. The low intensity region seen between the LII and the acetone fluorescence corresponds to the location where the parent fuel has come in contact with the hot products and undergone pyrolysis. Upon closer inspection it can be seen that the soot signal forms a connected region that borders the acetone signal.

Upon examination of the entire set of images for both propane and DME flames it was discovered that the LII signal was always present, and spatially separated from the OH region such that it could be clearly distinguished. The LII signal was also found to be an excellent marker of the parent fuel entrainment and of the internal structures of the mixing layer. As a result, the collection filter combination for a particular case was chosen to provide the best visualization of both the OH and LII.

Shown in Fig. 3 is a schematic illustrating the dominant features for both the air high-speed (AHS) and fuel high-speed (FHS) cases. These cases have identical inlet conditions, except that the high- and low-speed compositions are switched. In both FHS and AHS cases the mixing layer appeared to consist of two regions: a high temperature reaction zone with a fairly laminar appearance found on the oxidizer side of the mixing layer and an 'internal' mixing layer

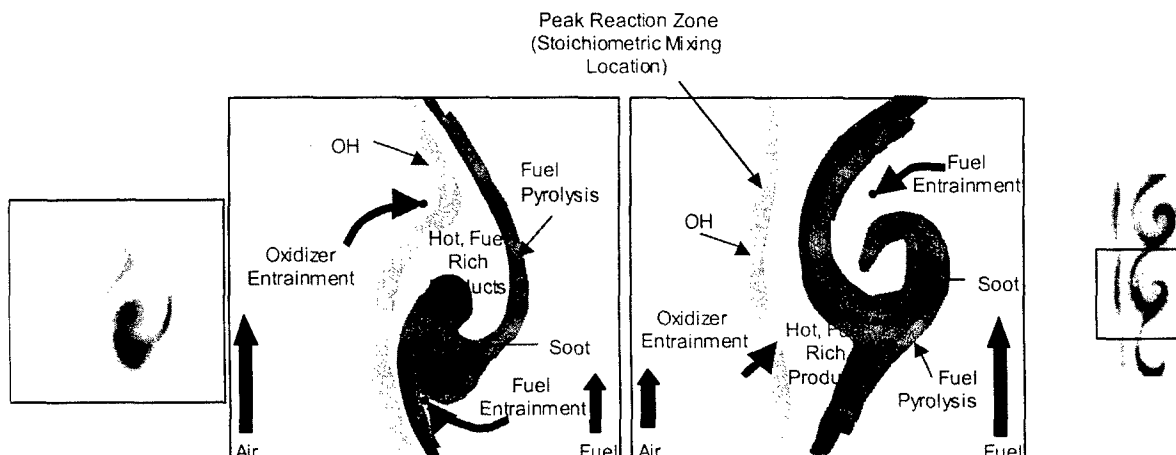


Figure 3 Schematic of the mixing layer structure for air on the high speed (left) and fuel on the high speed (right). Conditions are the same as Figure 2 except the fuel was propane.

in which products mix with pyrolyzed fuel in a manner reminiscent of a non-reacting two-stream mixing layer. The reaction zone seems only mildly influenced by the dynamics of the mixing layer. However, the processes affecting soot formation appear closely tied to the behavior of the mixing layer with a strong dependence upon the motion of the structures.

Figure 4 shows a direct comparison of the AHS and FHS operation with the non-reacting case shown as a reference. As in previous images, the OH signal is found to the left and the LII signal is found to the right. It is evident that the AHS cases have a much larger structure spacing than the FHS cases, and that the non-reacting case is intermediate to the two limits. This was a consistent result for all of the data sets acquired. Changes in the state of the high-speed boundary layer were unable to explain the magnitude of the effect that was observed.

The cause for the observed change in the observed instability wavelength is believed to be the result of the effective density profile that results from the combustion heat release. Since the stoichiometric mixture fraction is low, the flame will always be located on the air side of the mixing layer. The high temperature associated with the flame causes the air side to be lower in density. In the AHS case this causes the high-speed stream to have a lower density, and in the FHS case the low-speed stream density will be lower. A linear stability analysis performed by Trounev *et al.*¹, in which a hyperbolic tangent profile was assumed for both the inlet velocity and density profiles, showed that the low-density high-speed configuration produces an increase in instability wavelength, while the low-density low-speed configuration produces a decrease in the instability wavelength. This is consistent with the results shown in Figure 4.

The effects of heat release are expected to change the vorticity dynamics of the structures as well as modifying the gas properties of the mixing layer. However, to a first order, the dilation effect in vorticity reduction and the increase in viscosity associated with the heat release from the combustion are the same for the FHS and AHS cases (the adiabatic flame temperature is identical in both cases). While these effects, long considered to be important in jet flames, are believed to be important in both FHS and AHS cases, they do not account for the large differences in the instability wavelength.

The effect of tripping the high-speed boundary layer was found to have little discernible effect on the reacting structure (space constraints limit this discussion), but strongly affected the passive scalar results. Thus, the initial Kelvin-Helmholtz instability appears to be enhanced by the heat release.

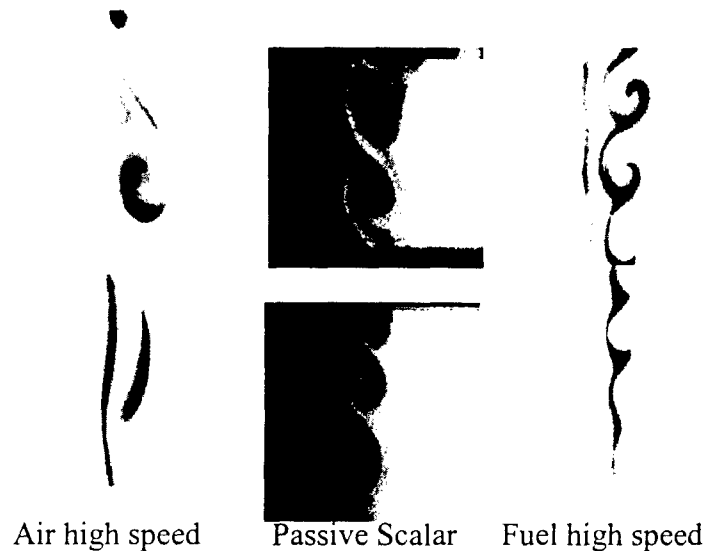


Figure 4 Comparison of reacting cases with non-reacting passive scalar images at the same inlet conditions. The air is on the left side in all images. The images are from positions A (lower) and B (upper) and the conditions are the same as Figure 3.

¹ Trounev, A., Candel, S.M. and Daily, J.W. AIAA Paper 88-0149, (1988).